CWP-110
June 1991

Three-Dimensional Explicit Depth Migration via McClellan Transformations on Hexagonal Sampling Grids

by

Justin P. Hedley

— Master's Thesis —

Supported through a fellowship granted by Chevron
Oil Field Research Company.

Center for Wave Phenomena
Colorado School of Mines
Golden, Colorado 80401
(303)273-3557

Three-dimensional Explicit Depth Migration via McClellan Transformations on Hexagonal Sampling Grids

Justin P. Hedley

ABSTRACT

The computational cost of three-dimensional depth migration depends almost entirely on the cost of depth extrapolation.

Each frequency of a 3-D seismic wavefield can be extrapolated by two-dimensional filters that vary spatially according to frequency and velocity. 2-D extrapolation filters are efficiently designed and implemented by use of McClellan transformations. McClellan transformations convert 1-D extrapolation filters to approximately circularly symmetric 2-D extrapolation filters at computational cost that is proportional to the number of unique coefficients, N, in the 1-D extrapolation filters. In contrast, the cost of direct convolution of 2-D extrapolation filters is proportional to N^2. Imaging of steep dips requires long extrapolation filters, i.e., large N, making direct 2-D convolution very expensive.

Although efficient, McClellan transformations only approximate circularly symmetric 2-D filters for depth extrapolation. The accuracy of a 2-D extrapolation filter can be improved only at an increase in the cost of implementing that filter.

By applying McClellan transformations on a hexagonal sampling grid, the accuracy of 2-D extrapolation filters can be improved at a reduction in cost. Furthermore, hexagonal sampling grids are the most efficient for spatially circularly band-limited seismic data, reducing the number of samples that are repeatedly processed during recursive depth extrapolation.

INTRODUCTION

Migration of seismic data is a process that maps reflections recorded on the earth to their origin, the subsurface reflectors. The result of migration is an image of the earth's interior.

Many migration algorithms, including the one presented in this thesis, separate the process into two steps, depth extrapolation followed by imaging. Depth extrapolation defines the seismic wavefield recorded at the earth's surface for all depths. Imaging is performed by evaluating the extrapolated wavefield at zero time.

The high computational cost of depth extrapolation requires efficient, yet accurate, algorithms. This thesis describes an efficient algorithm for accurate depth migration of post-stack, three-dimensional (3-D) seismic wavefields.

Since finite-difference methods for depth extrapolation can readily accommodate lateral velocity variations, they are commonly used for depth migration. Finite-difference depth extrapolation of stacked, two-dimensional (2-D) seismic wavefields is typically accomplished by an implicit numerical solution of an approximation to a one-way, paraxial wave equation (e.g. Claerbout, 1985). An attractive feature of implicit depth extrapolation methods is that they are unconditionally stable.

Unfortunately, implicit finite-difference methods are not easily extended to depth extrapolation of 3-D seismic wavefields. Claerbout (1985, p. 100-101) demonstrates that implicit numerical solutions for 3-D, finite-difference depth extrapolation are currently too computationally expensive to be practical. Splitting the 3-D depth extrapolation into a series of 2-D depth extrapolations in the in-line and cross-line directions enables a computationally efficient algorithm. However, Brown (1983), Yilmaz (1987, p. 405) and others have noted that splitting yields significant error near any 45-degree azimuth between the in-line and cross-line directions for reflector dips greater than about 20 degrees.

To reduce errors due to splitting, Ristow (1980) suggested further splitting along a 45-degree azimuth between the in-line and cross-line directions, a technique which significantly increases computational cost and complexity. Li (1990) proposed the addition of a phase-shift error-compensation operator to the split implicit algorithm. Accurate imaging in the presence of lateral velocity variations requires the use of phase-shift plus interpolation, which, again, significantly increases the computational cost and complexity of depth extrapolation.

Since explicit depth extrapolation of 3-D wavefields requires no splitting, perhaps explicit methods should be considered as an alternative to devising ways to improve the accuracy of split, implicit depth extrapolation. Unlike implicit depth extrapolation methods, explicit methods are not unconditionally stable. However, Holberg (1988) and Hale (1990a) have derived methods for stable *explicit* depth extrapolation of 2-D wavefields.

Three-dimensional explicit depth extrapolation can be performed for each frequency, ω, by convolution with spatially varying, *two-dimensional* filters. The velocity, v, determines the filter to be convolved with the data to extrapolate the wavefield in depth. A circularly symmetric filter, $h[n_x, n_y]$, for depth extrapolation should have a Fourier transform, $H(k_x, k_y)$, that approximates the desired Fourier transform, $D(k_x, k_y)$. That is,

$$H(k_x, k_y) \approx D(k_x, k_y) \equiv \exp\left[i\Delta z\sqrt{\frac{\omega^2}{v^2} - k_x^2 - k_y^2}\right], \tag{1}$$

where k_x and k_y are the in-line and cross-line wavenumber, respectively, and Δz is the depth-step size. (Throughout this thesis, I will denote a discretely sampled function by [ ] and a continuous function by ( ) . For example, $H(k_x, k_y)$ is the continuous Fourier transform of the sampled function, $h[n_x, n_y]$.) The desired Fourier transform in equation (1) is the familiar Gazdag phase-shift operator for post-stack depth extrapolation (Gazdag, 1978). The desired Fourier transform corresponds to waves travelling one-way, either up or down. Employing the "exploding reflectors" concept (e.g., Claerbout, 1985) requires the selection of upgoing waves. To match travel times of the real seismic experiment, the velocity used in depth extrapolation should be one-half the velocity of the medium.

Blacquière et al. (1989) designed filters for stable, explicit depth extrapolation of 3-D wavefields by a constrained least-squares method. This filter-design method was originally proposed by Holberg (1988) for stable, explicit depth extrapolation of 2-D wavefields. Both Blacquière et al. (1989) and Holberg (1988) demonstrated the validity of performing depth migration by spatially varying the filters according to ω/v, the ratio of frequency to velocity, in equation (1). However, calculating the filter coefficients for each frequency and velocity during depth extrapolation would be prohibitively slow. Instead, the filter coefficients are precalculated and stored in a table for numerous values of ω/v.

Although more accurate than splitting, the explicit depth extrapolation method of Blacquière et al. is also more expensive. If splitting was applied to explicit depth extrapolation, the computational cost would be proportional to N— the number of unique coefficients in the one-dimensional (1-D) filters used for 2-D depth extrapolation. In contrast, the cost of convolving 2-D filters for 3-D depth extrapolation is proportional to N^2. Hale (1990a) noted that, for explicit depth extrapolation of 2-D wavefields, accurate imaging of steep dips requires filters with $N \approx 40$ coefficients. Since the cost of explicit depth extrapolation without splitting is proportional to N^2, imaging steep dips in 3-D depth migration will be expensive.

To reduce computational costs and yet retain the accuracy of the explicit method, Hale (1990b) used McClellan transformations. McClellan transformations enable the design and implementation of approximately circularly symmetric filters for depth extrapolation at a cost proportional to N. Depth extrapolation via McClellan trans-

formations requires only 1-D filter coefficients of the type proposed by Holberg (1988) and Hale (1990a) for explicit depth extrapolation of 2-D wavefields.

McClellan transformations only approximate circularly symmetric filters for depth extrapolation. In this thesis, I will show that a more accurate approximation can be made by applying McClellan transformations on a hexagonal sampling grid. In addition, the combination of McClellan transformation and hexagonal sampling grids can further reduce the computational cost of explicit depth extrapolation in 3-D migration.

3-D EXPLICIT DEPTH MIGRATION VIA MCCLELLAN TRANSFORMATIONS

Introduction to McClellan transformations

Depth extrapolation of 3-D wavefields can be performed *explicitly* by convolution with spatially varying 2-D filters in order to avoid the errors associated with split *implicit* methods. However, 2-D convolution is computationally expensive. McClellan transformations can be used to combine the design and implementation of filters for depth extrapolation into one computationally efficient process.

McClellan transformations convert a symmetric 1-D filter for depth extrapolation of 2-D wavefields to an approximately circularly symmetric 2-D filter for depth extrapolation of 3-D wavefields at a computational cost that is less than direct 2-D convolution. Any 1-D extrapolation filters of the type proposed by Holberg (1988) and Hale (1990a) are valid for depth extrapolation via McClellan transformations.

A sampled, symmetric 1-D filter, $h[n]$, has a Fourier transform,

$$H(k) = \sum_{n=0}^{N-1} h[n](2 - \delta[n]) \cos(nk), \tag{2}$$

where N is the number of unique coefficients in that filter. The $\cos(nk)$ can be represented by an *nth* order Chebyshev polynomial (e.g., Abramowitz, M. and Stegun, I. A., 1965, p. 776),

$$T_n(\cos(k)) \equiv \cos(nk). \tag{3}$$

The polynomial is defined by the Chebyshev recursion,

$$T_n(\cos(k)) = 2\cos(k)T_{n-1}(\cos(k)) - T_{n-2}(\cos(k)), \tag{4}$$

where

$$T_0(\cos(k)) = 1,$$

and

$$T_1(\cos(k)) = \cos(k).$$

The Fourier transform of equation (2) can now be computed recursively from $\cos(k)$, so that

$$H(k) = h[0] + 2h[1]\cos(k) + 2h[2](2\cos(k)\cos(k) - 1) + \ldots \quad . \tag{5}$$

As an alternative to 1-D convolution, McClellan and Chan (1977) suggested that the filter of equation (5) could be implemented recursively by using the Chebyshev filter structure of Figure 1.

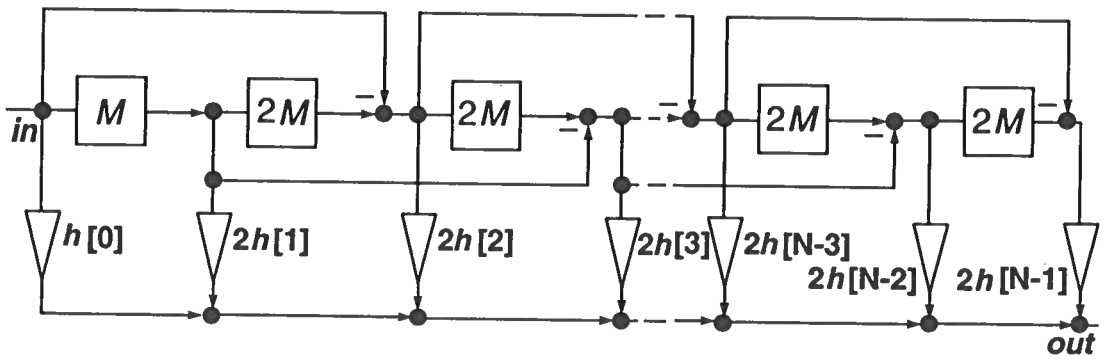

FIG. 1. Chebyshev filter-implementation structure.

The inverse Fourier transform of $M = M(k) \equiv \cos(k)$ is the short filter,

$$m[n] = \frac{1}{2}\delta[n+1] + \frac{1}{2}\delta[n-1], \tag{6}$$

which is repeatedly convolved with the data to be filtered. For 1-D filters, the computational cost of the Chebyshev filter structure exceeds that of direct convolution and is therefore not practical.

However, for circularly symmetric filters, where $k = \sqrt{k_x^2 + k_y^2}$, substituting $M(k_x, k_y)$ $\equiv \cos(\sqrt{k_x^2 + k_y^2})$ in the Chebyshev filter structure would enable the design and implementation of an exactly circularly symmetric 2-D filter from a 1-D filter. Unfortunately, the computational cost would again exceed that of direct 2-D convolution because the sampled filter, $m[n_x, n_y]$, corresponding to $M(k_x, k_y)$, would require a large number of coefficients.

To enable the *efficient* design and implementation of an approximately circularly symmetric filter, McClellan (1973) proposed the following approximation,

$$M(k_x, k_y) \equiv \cos(\sqrt{k_x^2 + k_y^2}) \approx A + B\cos(k_x) + C\cos(k_y) + D\cos(k_x)\cos(k_y), \tag{7}$$

where $-A = B = C = D = \frac{1}{2}$. The inverse Fourier transform of McClellan's original transformation in equation (7) is the compact 2-D filter of Figure 2.

$\frac{1}{8}$	$\frac{1}{4}$	$\frac{1}{8}$
$\frac{1}{4}$	$\frac{-1}{2}$	$\frac{1}{4}$
$\frac{1}{8}$	$\frac{1}{4}$	$\frac{1}{8}$

FIG. 2. Original McClellan transformation filter.

Because there are N stages in Figure 1, the cost of implementing a 2-D filter from a 1-D filter using McClellan transformations is linearly proportional to N—the number of unique coefficients in the 1-D filter. For some N, the cost will be proportional to the cost of convolving the original McClellan transformation filter with the data, which is 22 floating point operations (FLOPS) per grid point. Note that for the spatially varying filters required in depth extrapolation, only the 1-D filter coefficients, $h[n]$, will vary spatially. The coefficients of the McClellan transformation filter are constant.

Although computationally efficient, McClellan transformations only *approximate* circular filters for depth extrapolation by mapping the wavenumber response of the 1-D filter to the second dimension along approximately circular iso-wavenumber contours. Solving equation (7) for k_y gives

$$k_y = \arccos\left(\frac{2\cos(k) + 1 - \cos(k_x)}{1 + \cos(k_x)}\right). \tag{8}$$

Each wavenumber k defines a contour in the k_x, k_y domain. Along this curve the 2-D wavenumber response is constant and equal to the 1-D wavenumber response. Varying k from 0 to π yields the mapping of Figure 3.

The parameters, A, B, C, and D of equation (7) control how the McClellan transformation will approximate circular iso-wavenumber contours. Expressing the transformation in terms of sines will help clarify how each parameter can be selected to produce the same mapping as McClellan's. Using the half-angle formula,

$$\sin^2\left(\frac{\sqrt{k_x^2 + k_y^2}}{2}\right) \approx A' + B'\sin^2\left(\frac{k_x}{2}\right) + C'\sin^2\left(\frac{k_y}{2}\right) + D'\sin^2\left(\frac{k_x}{2}\right)\sin^2\left(\frac{k_y}{2}\right). \tag{9}$$

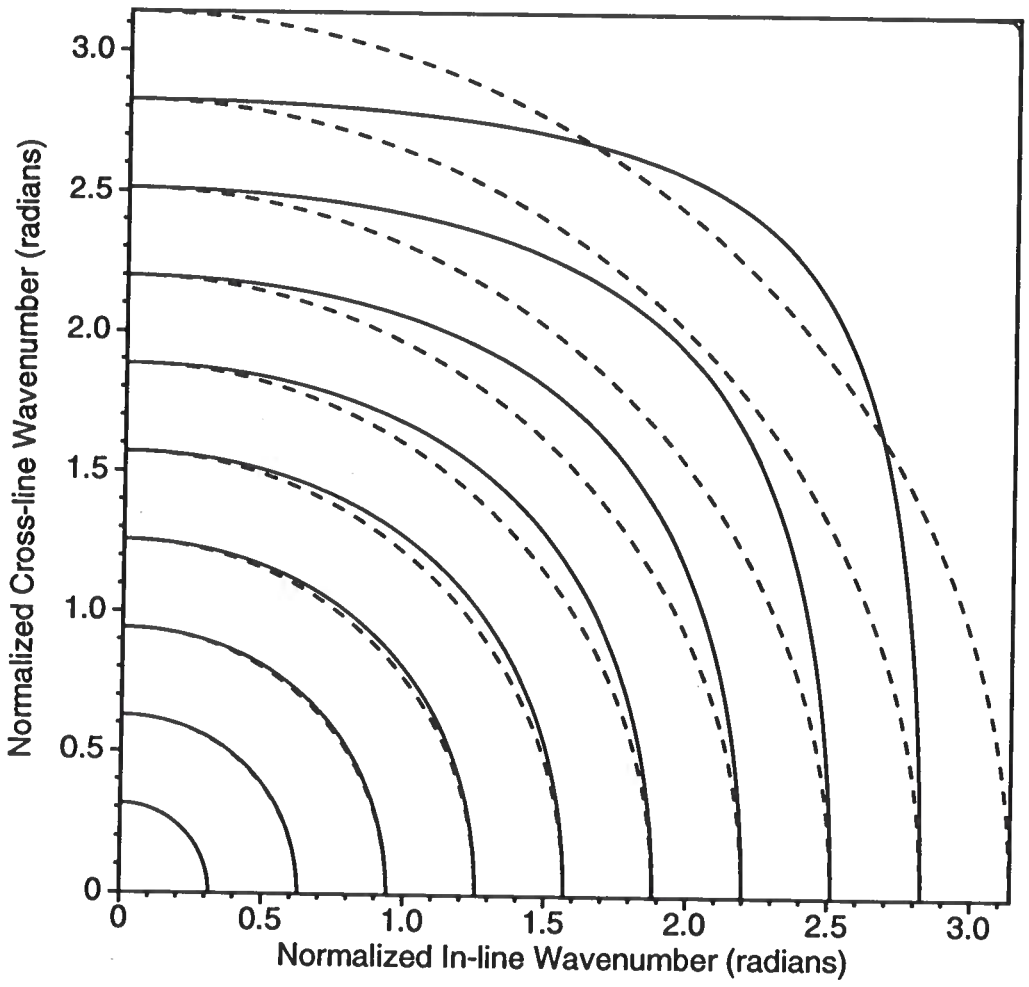

FIG. 3. The original McClellan transformation maps the wavenumber response of the 1-D filter to the second dimension along the solid contours. Dashed contours represent an exact circular mapping. Due to quadrantal symmetry, only the first quadrant is shown.

Note that the sine functions are monotonically increasing from 0 to π (normalized Nyquist frequency). Approximating for small k_x and k_y gives

$$k_x^2 + k_y^2 \approx 4A' + B'k_x^2 + C'k_y^2. \tag{10}$$

Referring to equations (9) and (10), observe that setting $A' = 0$ matches the origin of the 1-D filter, $k = 0$, to the 2-D origin, $k_x = k_y = 0$, and that $B' = C' = 1$ matches the 1-D filter exactly along the k_x and k_y axes and produces approximately circular contours for small k_x and k_y. Although not obvious, setting $D' = -1$ forces the outermost contour, $k = \pi$, to be square, which ensures that the approximation is within the range, $-1 \leq \sin^2(k/2) \leq 1$, so that the mapping will be defined for all k_x and k_y. However, forcing the outermost contour to be square also causes increasing contour error along $k_x = k_y$ (Figure 3), a 45 degree azimuth between the in-line and cross-line directions. Substituting the parameters, $A' = B' = C' = -D' = 1$, in equation (9) and expressing this equation in terms of cosines will give the parameters originally proposed by McClellan for equation (7).

Note that changing the parameters in the McClellan transformation will not affect the size of the transformation filter. Since McClellan did not select these parameters for depth-extrapolation filters, a different set parameters might be found that would enable the design of more accurate filters at the same computational cost. The parameters B' and C' cannot be modified because a 2-D filter for depth extrapolation should be correct along the k_x and k_y axes. Allowing $D' > -1$ would push the outermost contour along the diagonal towards the origin, thereby producing more nearly circular contours while also matching the 1-D filter exactly along the k_x and k_y axes. However, a region will then exist for which the contours are undefined. In Appendix A, I demonstrate that, in this region, the resulting 2-D extrapolation filter is highly unstable.

For extrapolation filters, the use of more parameters is required to improve the mapping of the 1-D filter in the wavenumber domain. Mersereau, et al. (1976) generalized the McClellan's approximation to

$$\cos(k) \approx \sum_{p=0}^{P} \sum_{q=0}^{Q} t[p,q] \cos(pk_x) \cos(qk_y). \tag{11}$$

where, $t[p,q]$, are the parameters of the transformation. Increasing the number of parameters may produce a more accurate extrapolation filter, but it will also increase the size of the McClellan transformation filter and thereby increase computational costs.

Hale (1990b) used an extra parameter to force the contours of the approximation to match exactly along the diagonal, $k_x = k_y$, at $\pi/3$. The result is the mapping illustrated in Figure 4.

Although Hale's improved McClellan transformation gives a better overall approximation to circular contours, the extra parameter increases the size of the transfor-

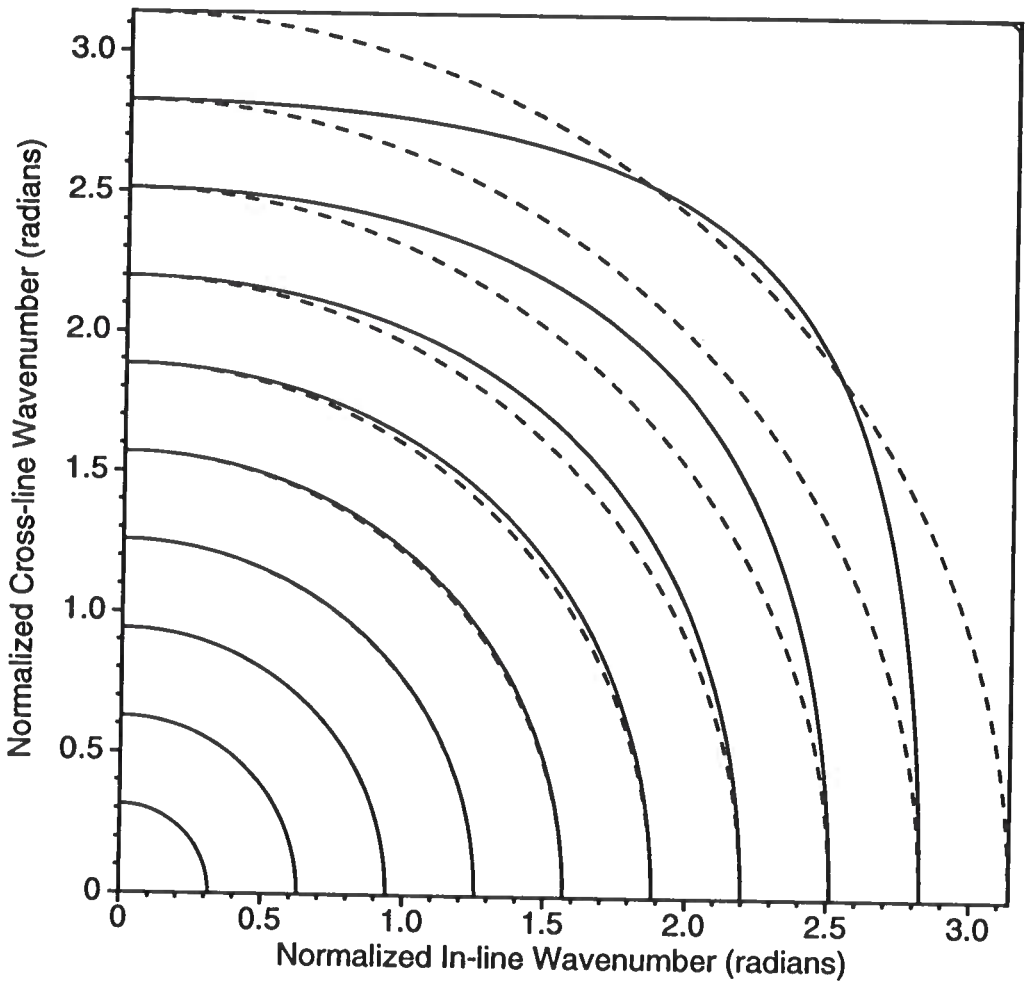

FIG. 4. Hale's improved McClellan transformation maps the wavenumber response of the 1-D filter to the second dimension along the solid contours. Dashed contours represent an exact circular mapping.

mation filter to that shown in Figure 5. The cost of convolving this filter with the data is 42 FLOPS per a grid point.

$-\frac{c}{8}$	0	$\frac{c}{4}$	0	$-\frac{c}{8}$
0	$\frac{1}{8}$	$\frac{1}{4}$	$\frac{1}{8}$	0
$\frac{c}{4}$	$\frac{1}{4}$	$-\frac{1+c}{2}$	$\frac{1}{4}$	$\frac{c}{4}$
0	$\frac{1}{8}$	$\frac{1}{4}$	$\frac{1}{8}$	0
$-\frac{c}{8}$	0	$\frac{c}{4}$	0	$-\frac{c}{8}$

FIG. 5. Hale's improved McClellan transformation filter. $c \approx 0.0255$.

Three-dimensional depth migration via McClellan transformations

Hale (1990b) demonstrated the implementation of 3-D explicit depth migration via McClellan transformations by migrating an impulse over a limited band of frequencies.

The 3-D Fourier transform of a discrete impulse, $i[n_t, n_x, n_y] \equiv \delta[n_t, n_x, n_y]$, is

$$I(\omega, k_x, k_y) = 1 \quad |\omega| \leq \pi, \quad |k_x| \leq \pi, \quad |k_y| \leq \pi. \tag{12}$$

Note that the Nyquist frequency and wavenumbers are π radians. The function, I, for each frequency, ω, contains all wavenumbers, k_x and k_y, from $-\pi$ to π.

Errors of the McClellan transformations become significant for higher wavenumbers, which would suggest that the migration of an impulse by McClellan transformations would be inaccurate.

A wavenumber-filtering property of Hale's extrapolation filters can limit the wavenumbers of an impulse to be migrated to a range for which the McClellan transformations are accurate. Each of Hale's extrapolation filters act as a low-pass filter with a cut-off wavenumber,

$$k_{cutoff} \approx \frac{2\omega}{v} \sin(\theta_{max}) \tag{13}$$

where ω/v is the ratio of frequency to velocity and θ_{max} is the maximum propagation angle accurately handled by the extrapolation filter. Errors of the McClellan transformations in the reject band of the extrapolation filters have no effect on the final

migrated image. Longer extrapolation filters will handle steeper propagation angles. The 39-coefficient extrapolation filters used by Hale (1990b) to test migration via McClellen transformations will handle propagation angles up to about 50 degrees. For a constant-velocity, v, the maximum wavenumbers of an impulse to be migrated are limited by the maximum frequency to be migrated.

I will migrate a band-limited impulse with sufficiently high frequencies, in order to examine the relationship between errors in the McClellan transformations and errors in the migration impulses responses. For the tests, the sampling intervals are $\triangle x = \triangle y = \triangle z = 10$ m. The impulse is centered at $t = 0.46$ s. The velocity, v, is 2 km/s.

Figures 6 and 7 are in-line slices at a coordinate of $y = 0$ from the migration of an impulse over a frequency band of 0 to 45 Hz, using the original and Hale's improved McClellan transformations. From equation (13) the maximum cutoff wavenumber, normalized by the sampling interval, will be approximately 2.2 radians. There is little difference between these two figures, since for $k_y = 0$ both transformations produce an exact mapping up to the Nyquist wavenumber.

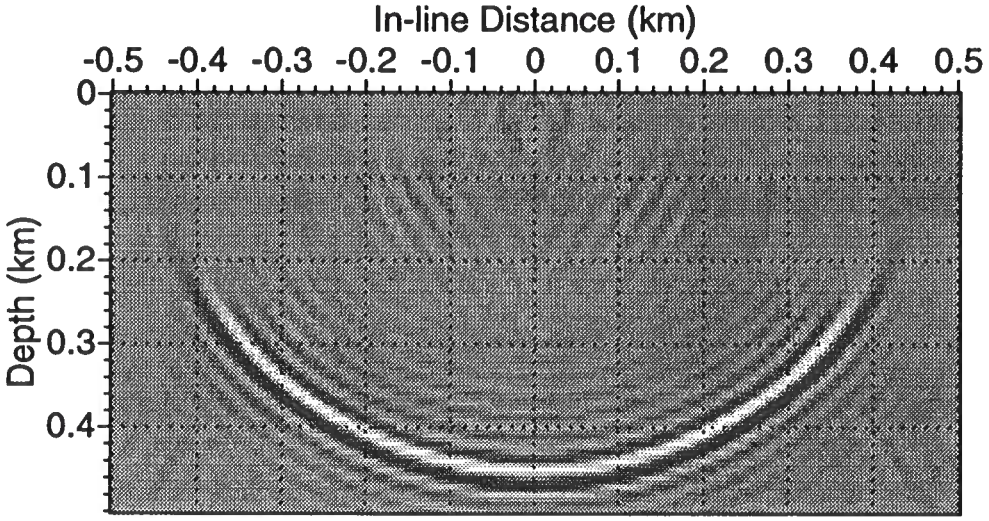

FIG. 6. In-line slice at $y = 0$ from an explicit depth migration of an impulse with a frequency range from 0 to 45 Hz, via the original McClellan transformation.

Figures 8 and 9, constant-depth slices at $z = 250$ m from the migration of an impulse by the original and Hale's improved McClellan transformations, illustrate the relationship between errors in the McClellan transformations and errors in the

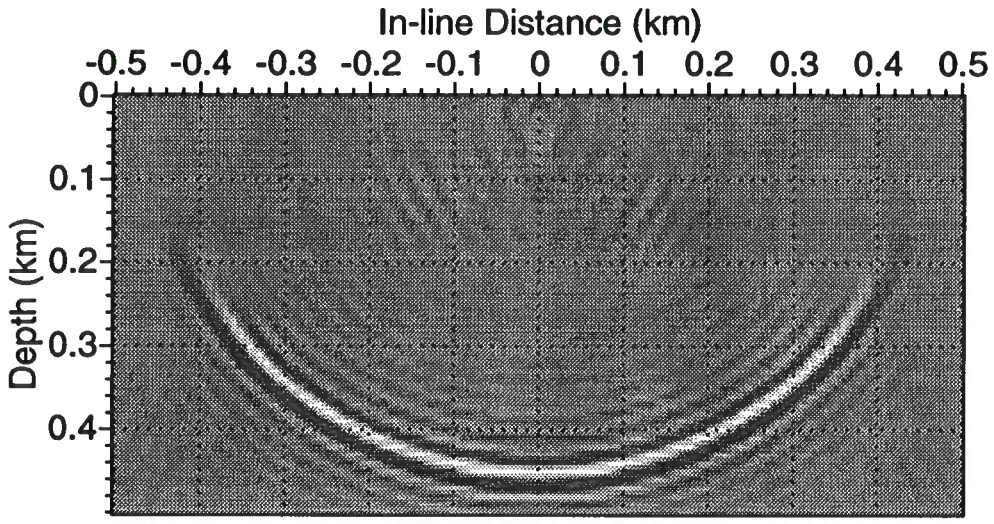

FIG. 7. In-line slice at $y = 0$ from an explicit depth migration of an impulse with a frequency range from 0 to 45 Hz via, Hale's improved McClellan transformation.

resulting migrations. By the similarity theorem (e.g., Bracewell, R. N., 1986, p. 101),

$$h(ax) \longleftrightarrow \frac{1}{|a|} H\left(\frac{k_x}{a}\right), \tag{14}$$

in the directions where the contours in the wavenumber domain have been stretched (Figures 3 and 4) the impulse responses of extrapolation filters with higher cutoff wavenumbers, k_{cutoff}, are compressed. Because the contour stretching is greatest for $k_x = k_y$, the compression of extrapolation filters yields a compression of the migration impulse responses that is greatest for $x = y$. Errors in the migration impulse responses thus correspond directly to contour error of the McClellan transformations, which explains why the migration impulse response for Hale's improved transformation (Figure 9) is more accurate than that for McClellan's original transformation (Figure 8).

Like splitting, 3-D migrations via McClellan transformations exhibit errors that are greatest at 45-degree angles between the in-line and cross-line directions. However, unlike splitting, McClellan transformations produce migration errors that are a function of wavenumber, *not* dip. Low frequencies, corresponding to low wavenumbers, are accurately migrated to the maximum propagation angle of the 1-D extrapolation filters by both transformations.

It has been demonstrated that although the original McClellan transformation is cheaper to implement than Hale's improved McClellan transformation, it is also less

accurate. Spatially oversampling the data could force its normalized band-region to overlap the region where the original McClellan transformation is accurate. However, probably little, if anything, would be gained since that would require that the data be resampled to a much finer grid. Instead, I propose resampling to a hexagonal grid, which has fewer samples than a corresponding rectangular grid and for which a McClellan transformation can be found that is almost as accurate as Hale's improved McClellan transformation, at a lower cost than that of the original McClellan transformation.

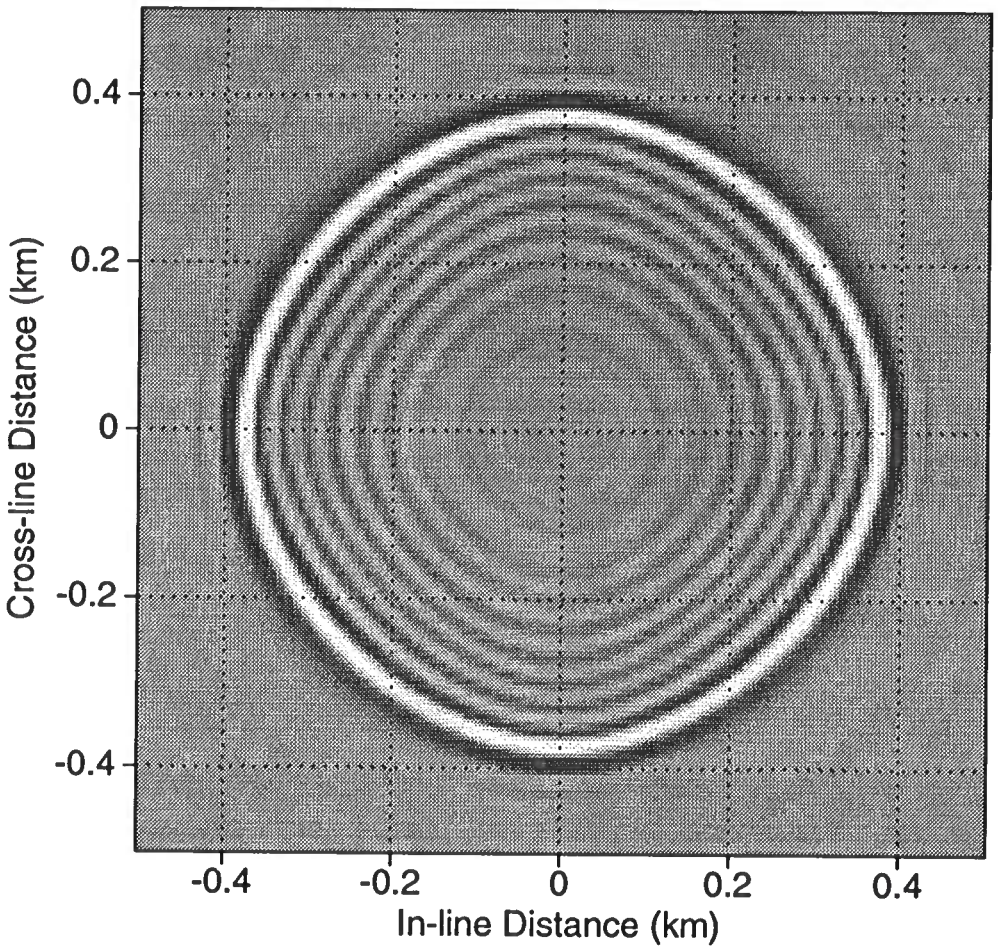

FIG. 8. Depth slice at $z = 250$ m from an explicit depth migration of an impulse with a frequency range from 0 to 45 Hz, via the original McClellan transformation.

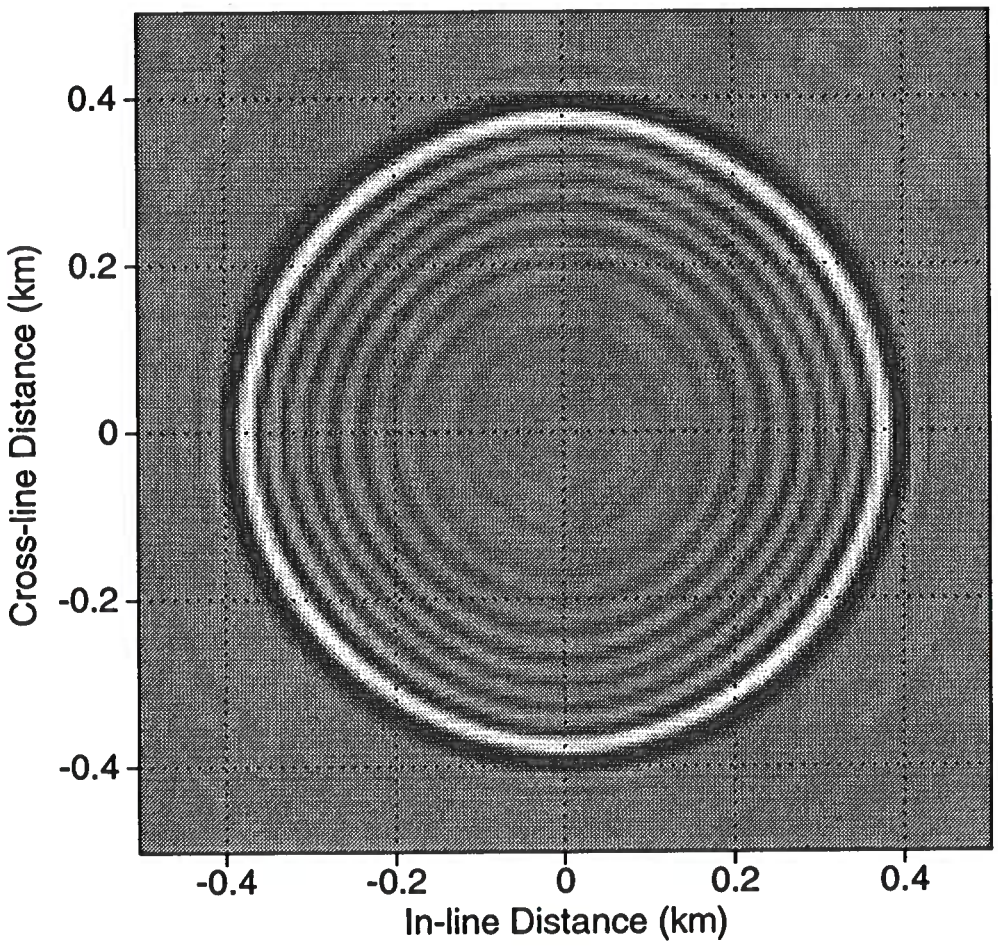

FIG. 9. Depth slice at $z = 250$ m from an explicit depth migration of an impulse with a frequency range from 0 to 45 Hz, via Hale's improved McClellan transformation.

3-D EXPLICIT DEPTH MIGRATION VIA HEXAGONAL MCCLELLAN TRANSFORMATIONS

Introduction to hexagonal sampling

It can be shown that the mean sampling density of a 2-D sampling grid is proportional to the area of the grid's corresponding shape (the *bandshape*) in the Fourier plane (Mersereau, 1979). The most efficient sampling grid for a particular waveform will have a bandshape that most closely approximates the waveform's bandregion (that region where the waveform's spectrum is non-zero) in the Fourier plane. To avoid aliasing, the grid's bandshape must contain the entire bandregion of the waveform.

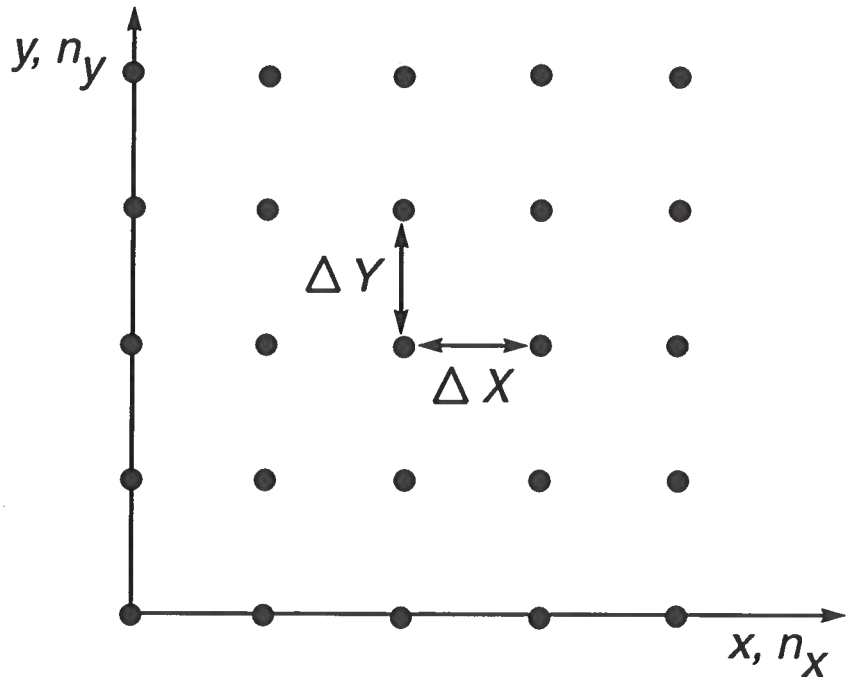

FIG. 10. Rectangular 2-D spatial sampling grid, where x and y are the continuous axes, and n_x and n_y are the discrete axes. ΔX and ΔY are the sampling intervals.

A frequency slice of the 3-D Fourier transform of stacked seismic data is spatially band-limited to a circular bandregion, assuming that previous processing has removed any evanescent energy; that is,

$$\sqrt{k_x^2 + k_y^2} \leq \frac{2\omega}{v_o} \tag{15}$$

where k_x and k_y are the in-line and cross-line wavenumbers, respectively, ω is the frequency, and v_o is the velocity at the recording surface.

A frequency slice of the 3-D Fourier transform of seismic data sampled on the traditional rectangular grid of Figure 10 will be contained in the rectangular bandshape of Figure 11. The normalized Nyquist wavenumbers, k_{xN} and k_{yN}, of the rectangular bandshape are π.

The same frequency slice, sampled on the hexagonal grid of Figure 12, will be contained in the hexagonal bandshape of Figure 13. Due to its smaller bandshape, a hexagonal grid requires 13 percent fewer samples than a rectangular grid to sample stacked seismic data. For circularly bandlimited waveforms, a hexagonal sampling grid is the most efficient (Mersereau, 1979).

Although there may be advantages to spatially recording and processing 3-D seismic data on a hexagonal sampling grid, in this thesis, I will be concerned only with issues involving the resampling of stacked 3-D seismic data between rectangular and

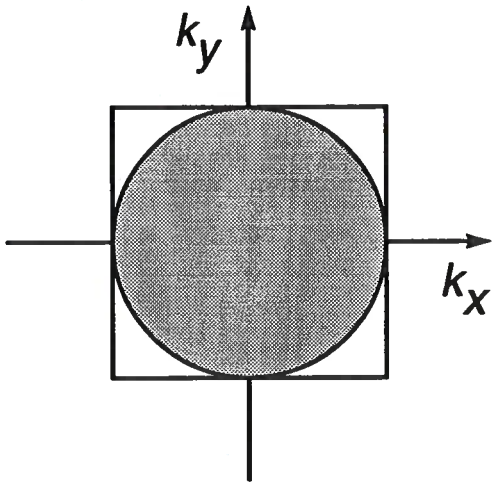

FIG. 11. Frequency slice of the 3-D Fourier transform of seismic data sampled on a rectangular grid. The rectangular grid forces the Fourier transform, which is band-limited to a circular bandregion, to be contained within a rectangular bandshape.

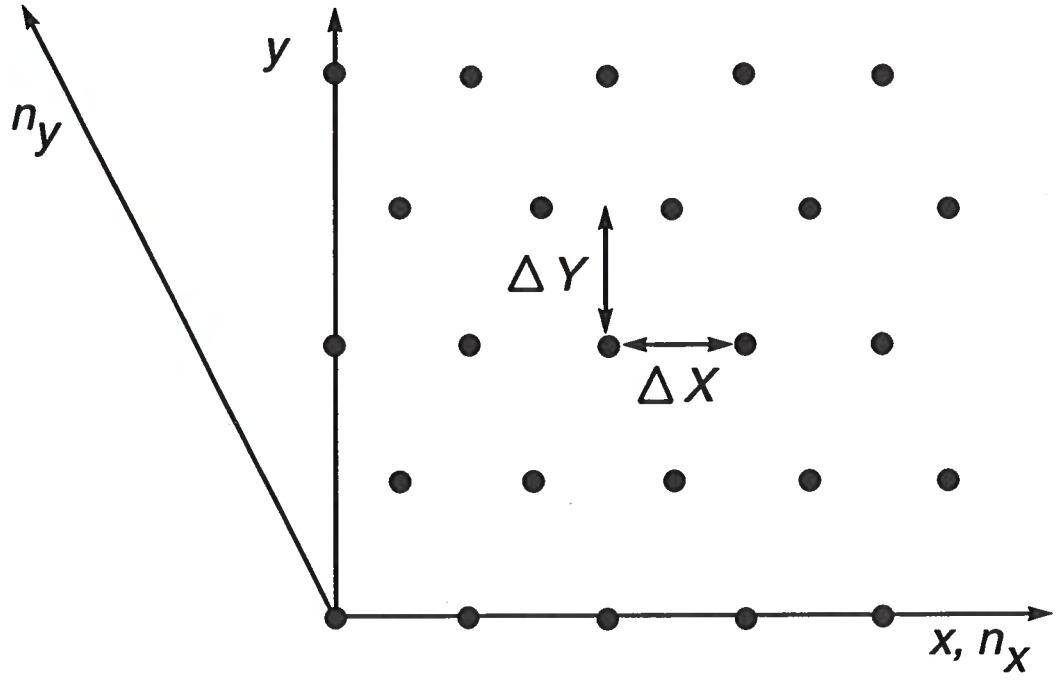

FIG. 12. Hexagonal 2-D sampling grid, where x and y are the continuous axes, and n_x and n_y are the discrete axes. ΔX and ΔY are the sampling intervals.

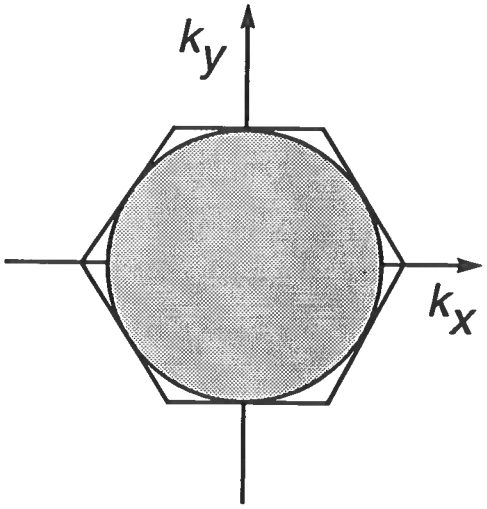

FIG. 13. The same frequency slice of the 3-D Fourier transform of seismic data sampled on a hexagonal grid. The bandshape of the hexagonal grid more closely approximates the bandregion of the frequency slice.

hexagonal grids. Please refer to Mersereau (1979) for a thorough discussion of the sampling of continuous waveforms on hexagonal grids.

Resampling to a hexagonal grid

To allow for vertical velocity variations, extrapolation filters extrapolate the wavefield in increments, each depth increment being a small fraction of the total depth, and over which the velocity is assumed to be constant. Depth migration on a hexagonal grid requires that each frequency slab of the wavefield be: (1) resampled to the hexagonal grid, (2) extrapolated for all depths, and then, (3) after all frequencies are accumulated, resampled to the rectangular grid. However, the cost of this resampling is small in comparison to the savings obtained by the reduction of samples in each frequency slab that have be repeatedly extrapolated to define the wavefield for all depths. In this thesis, I show that McClellan transformations on a hexagonal grid produce computational savings in addition to a reduction of samples.

Commonly, for 3-D seismic data, the cross-line sampling interval, Δy, is greater than the in-line sampling interval, Δx. Before migration, trace interpolation is often performed in the cross-line direction to overcome spatial aliasing. Trace interpolation in the cross-line direction, when necessary, *increases* the computational cost of migration by increasing the total number of samples to be processed. Once a sampling interval that prevents aliasing is obtained in the cross-line direction, hexagonal

gridding of each frequency slab of the data requires resampling *only* in the in-line direction.

Hexagonal sampling reduces the total number of samples by increasing the in-line sampling interval for all lines to

$$\Delta x_{hex} = \frac{2}{\sqrt{3}} \Delta x_{rect}. \tag{16}$$

Referring to Figure 12, note that the samples of every other in-line row are shifted by half the sampling interval, $\Delta x_{hex}/2$.

The sampling interval of equation (16) ensures the wavefield slab of maximum frequency will not be aliased during resampling, since, according to equation (15), each frequency slice of data is band-limited to a circle with a radius that is proportional to frequency. However, all other frequencies will be oversampled. Although not implemented in this thesis, a further reduction in samples could be obtained by dividing the wavefield into frequency groups for which coarser sampling may be used.

Hexagonal McClellan transformations

The McClellan transformation filters, the small 2-D filters that must be repeatedly convolved with the data during the Chebyshev implementation shown in Figure 1, should be circularly symmetric. Figure 14 illustrates that the impulse response of a digital filter on a hexagonal grid possesses twelve-fold symmetry, while on a rectangular grid it has only eight-fold symmetry. To represent circularly symmetric digital filters, a hexagonal grid is thus a more natural coordinate system than a rectangular grid.

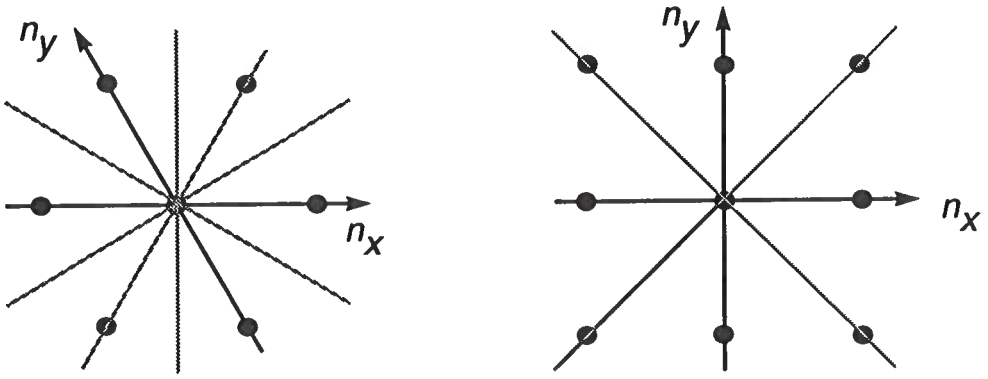

FIG. 14. A 2-D circularly symmetric filter represented on a hexagonal grid and a rectangular grid.

McClellan's original transformation on a hexagonal grid for circularly symmetric 2-D filters is

$$\cos(\sqrt{k_x^2 + k_y^2}) \approx M(k_x, k_y) = -A + B\left(\cos\left(\frac{2k_x}{\sqrt{3}}\right) + 2\cos\left(\frac{k_x}{\sqrt{3}}\right)\cos(k_y)\right) \quad (17)$$

where $A = -1/3$ and $B = 4/9$ (Mersereau, 1979). This approximation maps the wavenumber response of the 1-D extrapolation filter to the second dimension along the iso-wavenumber contours of Figure 15.

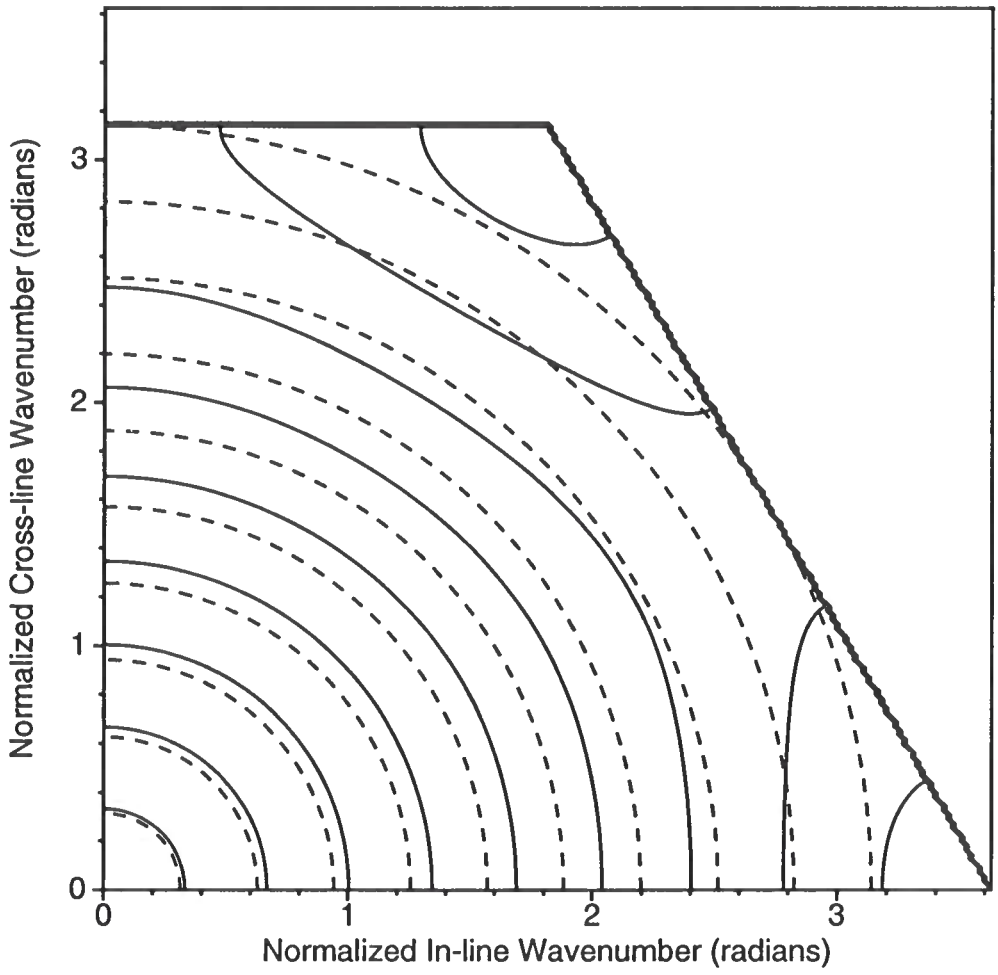

FIG. 15. The original hexagonal McClellan transformation maps the wavenumber response of the 1-D filter to the second dimension along the solid contours. Dashed contours represent an exact circular mapping.

The mapping of the original hexagonal McClellan transformation, although circular for lower wavenumbers, deviates from the desired mapping for all wavenumbers. This is illustrated by substituting the small angle approximation, $\cos(k) \approx 1 - k^2/2$, into equation (17) which gives

$$k_x^2 + k_y^2 \approx \frac{8k_x^2}{9} + \frac{8k_y^2}{9}. \tag{18}$$

The two parameters A and B cannot be modified to produce a better mapping for depth extrapolation filters. The parameter A matches the origin of the 1-D filter to the 2-D origin. The parameter B forces the contours of the approximation to be defined for all k_x and k_y which is a requirement for a stable 2-D filter. (See Appendix A.)

Referring to Figure 15 and equation (18), for small wavenumbers, the deviation of the actual contours from the desired contours is increasingly linearly. To compensate, I introduced a compression factor, α. The compressed original hexagonal McClellan transformation is

$$M(\alpha k_x, \alpha k_y) = -A + B\left(\cos\left(\frac{2\alpha k_x}{\sqrt{3}}\right) + 2\cos\left(\frac{\alpha k_x}{\sqrt{3}}\right)\cos(\alpha k_y)\right). \tag{19}$$

Selection of α forces the approximate and desired contours to match exactly along the k_x axis at some wavenumber. I selected $\alpha \approx 1.072$ to match exactly at $k_x = 5\pi/12$ to distribute contour error above and below that wavenumber, which produces the mapping of Figure 16. Figure 17 illustrates that the wavenumber mapping of the compressed original hexagonal McClellan transformation is almost as accurate as Hale's *improved* McClellan transformation.

In practice, the compression factor, α, does not become part of the transformation. To understand why, consider the inverse Fourier transform of the 1-D function, $F(k) = \cos(\alpha k)$, to the discretely sampled function

$$f[n] = \frac{\sin(\pi(n-\alpha))}{2\pi(n-\alpha)} + \frac{\sin(\pi(n+\alpha))}{2\pi(n+\alpha)}. \tag{20}$$

Only when α is an integer does equation (20) become the compact filter

$$f[n] = \frac{1}{2}\delta[n-\alpha] + \frac{1}{2}\delta[n+\alpha]. \tag{21}$$

Therefore, $\alpha \approx 1.072$ would distort the compact impulses into large sinc functions. The same reasoning holds true for the inverse 2-D discrete hexagonal Fourier transform. Compact McClellan transformation filters are required for the efficient implementation of 2-D filters.

Instead, a new table of 1-D extrapolation filters, with wavenumber responses that are compressed in proportion to α, are calculated. *No* modification of Hale's 1-D extrapolation design algorithm is required. For the design of compressed 1-D

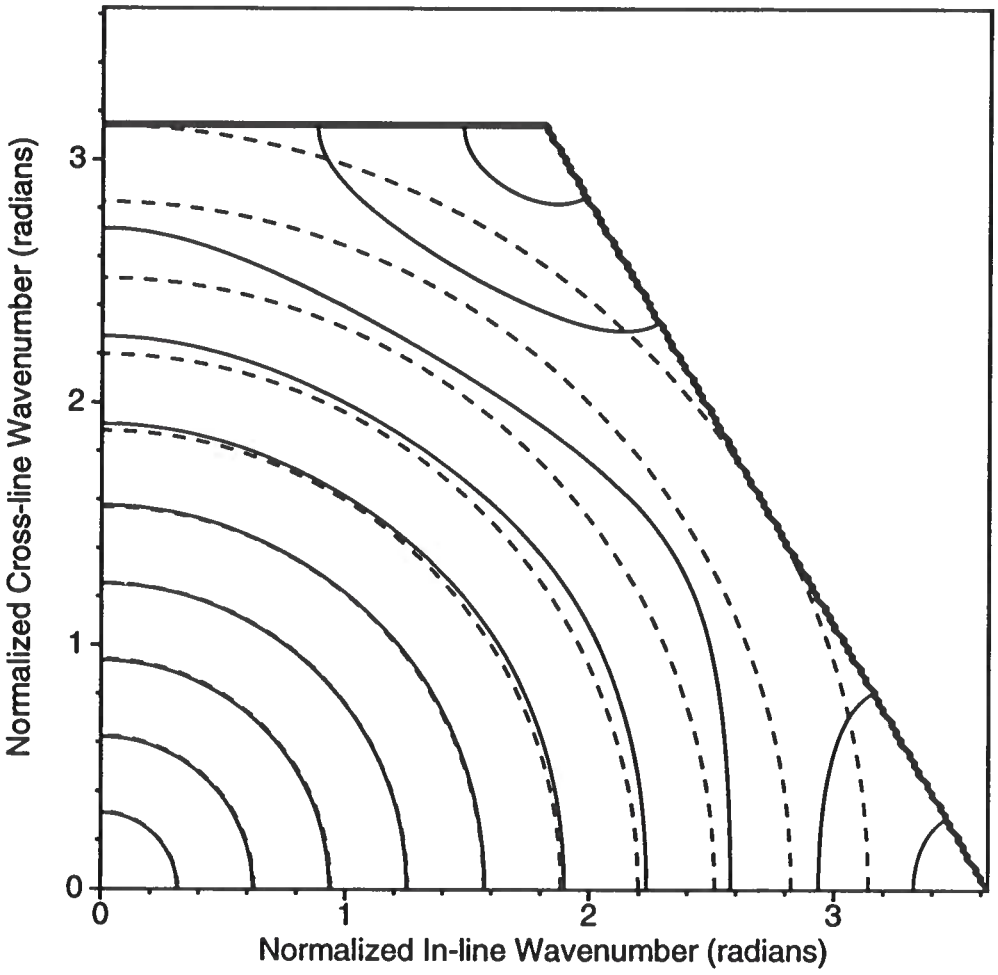

FIG. 16. The compressed original hexagonal McClellan transformation maps the wavenumber response of the 1-D filter to the second dimension along the solid contours. Dashed contours represent an exact circular mapping.

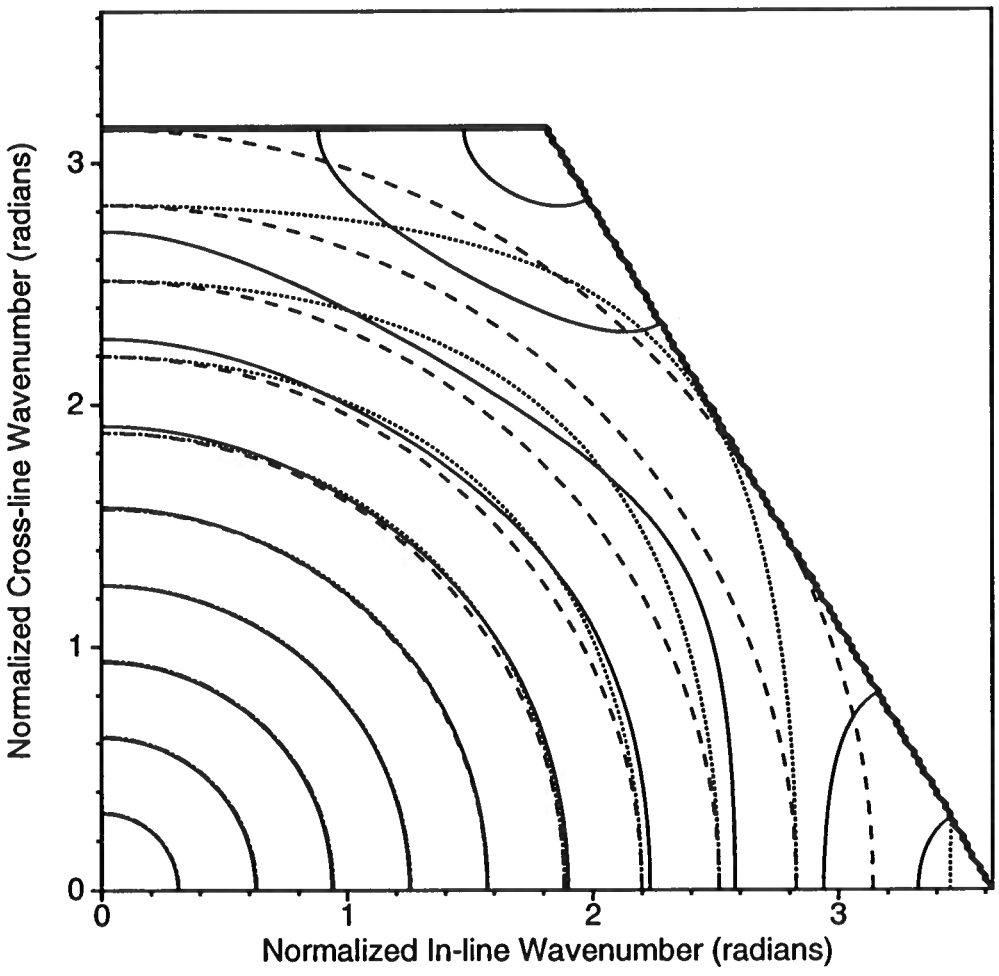

FIG. 17. Solid contours are the wavenumber mapping of the compressed original hexagonal McClellan transformation; dotted contours are the wavenumber mapping of Hale's improved McClellan transformation; and the dashed contours are an exact mapping.

extrapolation filters, the horizontal spatial sampling interval is specified as

$$\Delta x_{compressed\ design} = \frac{\Delta x_{design}}{\alpha}. \tag{22}$$

With this compression factor, the original hexagonal McClellan transformation is more accurate the original McClellan transformation. It is also less costly to implement. The inverse Fourier transform of the original hexagonal McClellan transformation is the filter of Figure 18. The hexagonal filter has only seven coefficients

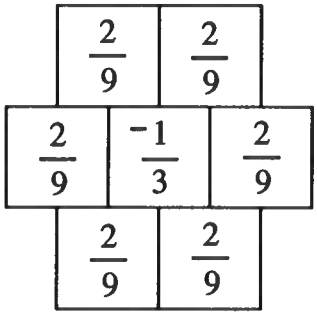

FIG. 18. Original hexagonal McClellan transformation filter.

(two unique) while the rectangular filter has 9 coefficients (three unique). The cost of convolving the hexagonal filter is 16 FLOPS per grid point, roughly 3/4 the cost of convolution with the rectangular filter.

As was true for the rectangular transformation filter, a more accurate approximation can be obtained by increasing the number of parameters in the hexagonal McClellan transformation. I derived a hexagonal McClellan transformation with a total of four parameters.

Since the compression factor, α, yields a better mapping along the k_x axis than the k_y axis, the two extra parameters were used to force the mapping along the k_y axis to match the mapping along k_x axis at $k_y = 0.4\pi$ and $k_y = 0.8\pi$. This allows α to have a more uniform action for all k_x and k_y. The resulting, highly circular contours, shown in Figure 18, of this improved hexagonal McClellan transformation are significantly more accurate than are the contours for Hale's improved transformation of Figure 4.

The inverse Fourier transform of the improved hexagonal McClellan transformation is the filter of Figure 20. The cost of convolving this filter with the data is 44 FLOPS per grid point, which is approximately the same as that of Hale's improved McClellan transformation filter.

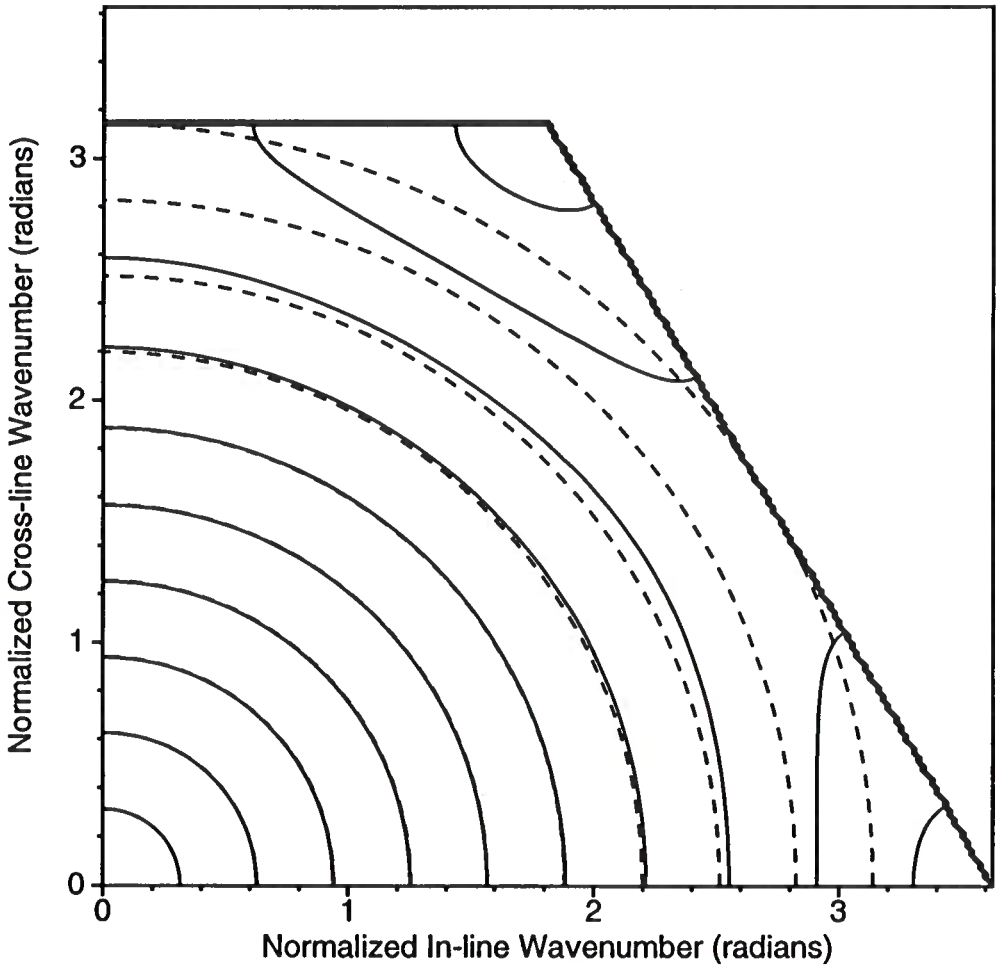

FIG. 19. The compressed improved hexagonal McClellan transformation maps the wavenumber response of the 1-D filter to the second dimension along the solid contours. Dashed contours represent an exact circular mapping.

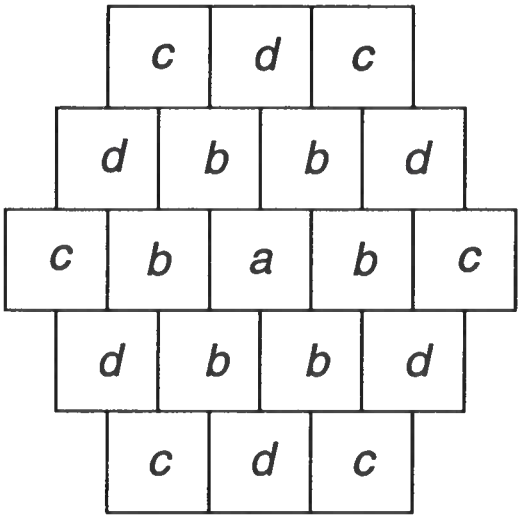

FIG. 20. Improved hexagonal McClellan transformation filter, where $a \approx -0.708$, $b \approx 0.454$, $c \approx -0.00942$ and $d \approx 0.00692$.

3-D migration via hexagonal McClellan transformations

To compare and contrast 3-D explicit depth migration via rectangular and hexagonal McClellan transformations, I migrated an impulse, band-limited to the same range of frequencies, 0 to 45 Hz, and with sampling intervals, $\triangle x = \triangle y = \triangle z = 10$ m, and velocity, v=2 km/s, as for the rectangular case. The maximum frequency to be migrated, 45 Hz, gives a maximum extrapolation filter cutoff wavenumber, $k_{cutoff} \approx 2.2$ radians.

To ensure against aliasing when resampling to the hexagonal grid, the impulse was modified to be spatially circularly band-limited since a discrete impulse is rectangularly band-limited (equation 12). The modified impulse, a 2-D discrete Jinc function (e.g., Bracewell, R. N., 1986, p. 422), is

$$\text{Jinc}[n_r] \equiv \frac{J_1[\pi n_r]}{n_r}, \tag{23}$$

where J_1 is a first order Bessel function, and $n_r = \sqrt{n_x^2 + n_y^2}$. Figure 21 shows the slice of the modified impulse at $t = 0.46$ s. Figure 22 is a slice, at $t = 0.46$ s, of the magnitude of the spatial Fourier transform of the modified impulse. The magnitude is approximately unity within the circular bandregion.

To resample the data to the hexagonal grid, I used an eight-point sinc interpolation routine, which produces a maximum error of less than 1 percent up to approximately 0.6 Nyquist.

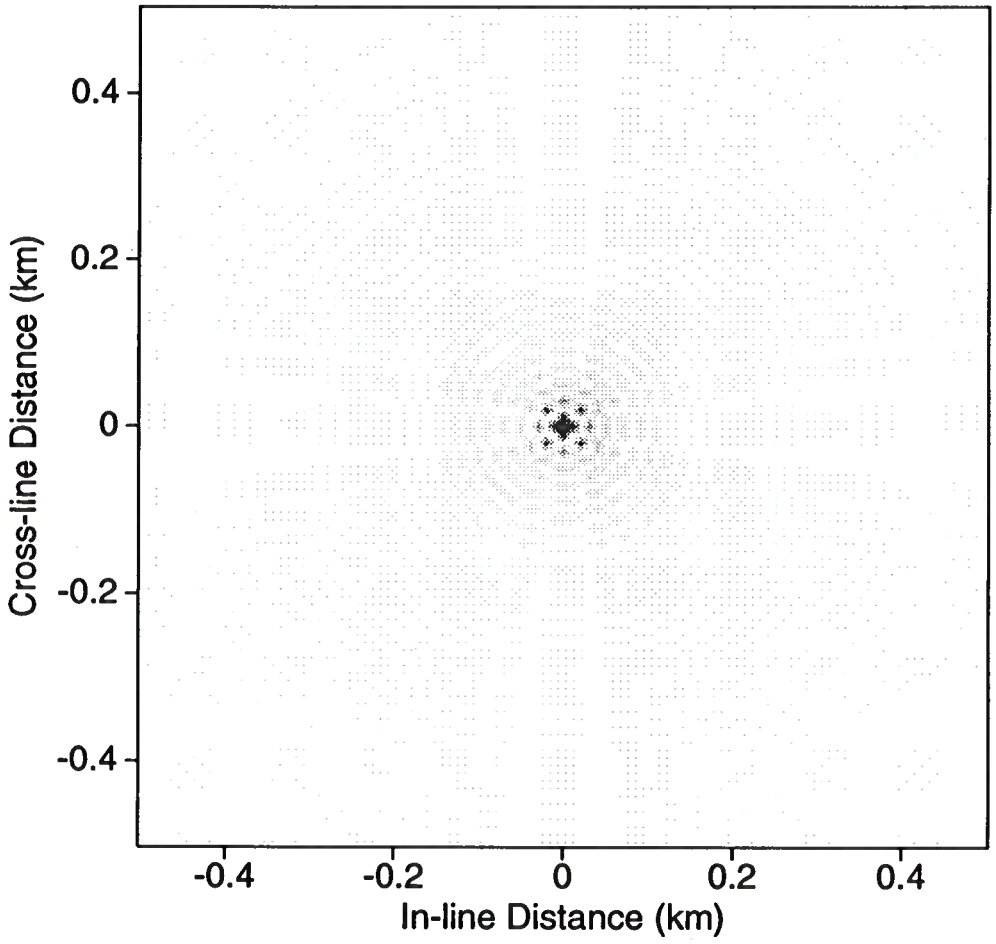

FIG. 21. Slice, at $t = 0.46$ s, of the modified impulse.

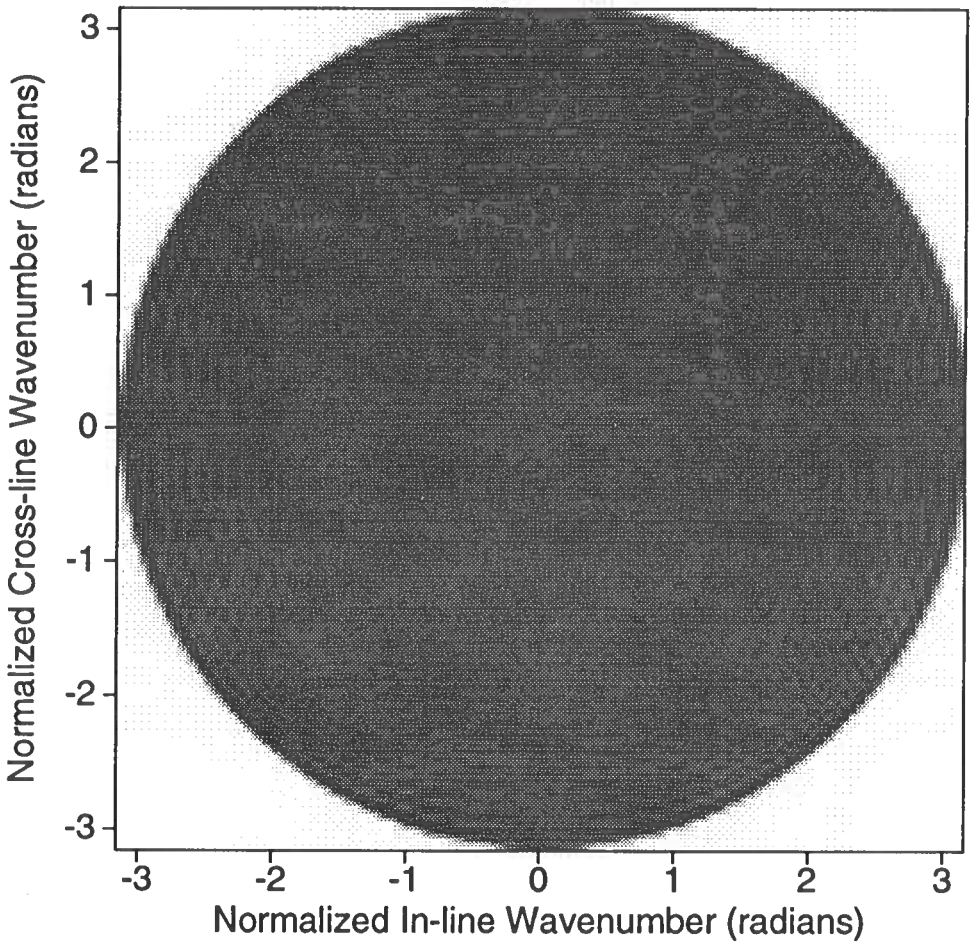

FIG. 22. Slice, at $t = 0.46$ s, of the spatial Fourier transform of the modified impulse.

Figures 23, 24 and 25 are in-line slices at $y = 0$ from the migration of an impulse using the original hexagonal, Hale's improved and the improved hexagonal McClellan transformations. As demonstrated previously, the errors in the 3-D migration impulse responses relate directly to errors in the mappings of the McClellan transformations. The original hexagonal McClellan transformation shows a slight compression of the impulse response, since, unlike Hale's improved rectangular transformation, the mapping is not exact for $k_y = 0$. If the original hexagonal transformation is considered to be accurate up to 1.9 radian than the improved hexagonal McClellan is accurate up to 2.2 radians, the maximum k_{cutoff} of the extrapolation filters.

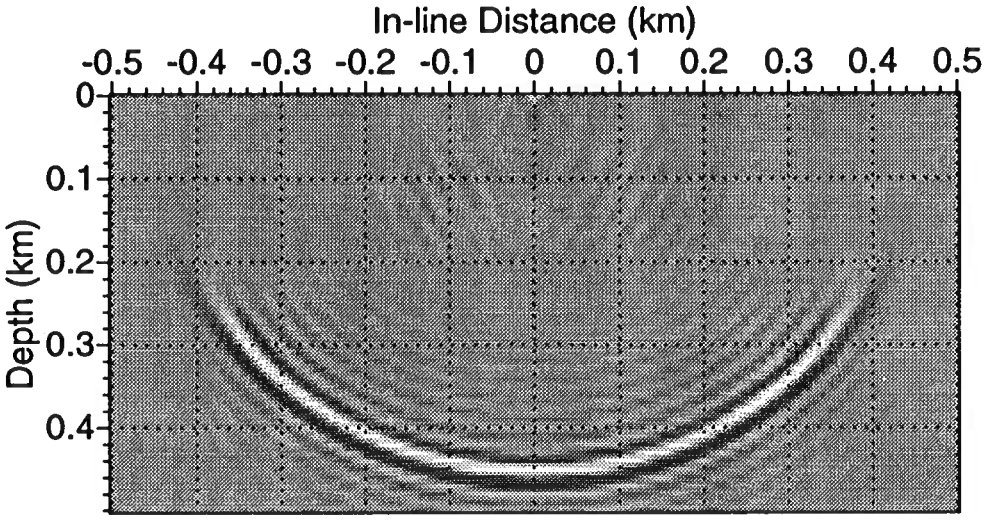

FIG. 23. In-line slice at $y = 0$ from an explicit depth migration of an impulse with a frequency range from 0 to 45 Hz, via the original hexagonal McClellan transformation.

Figures 26, 27 and 28 show depth slices at $z = 250$ m from the migration of an impulse by the original hexagonal, Hale's improved, and the improved hexagonal McClellan transformations. They demonstrate that the original hexagonal transformation compares very favorably, overall, to Hale's improved McClellan transformation. The improved hexagonal McClellan transformation is clearly the most accurate of the three.

CONCLUSION

3-D explicit depth migrations via McClellan transformations, both rectangular and hexagonal, are able to avoid the errors of split implicit methods without the high computational cost of 2-D explicit depth extrapolation filters.

McClellan transformations are better applied on hexagonal grids because:

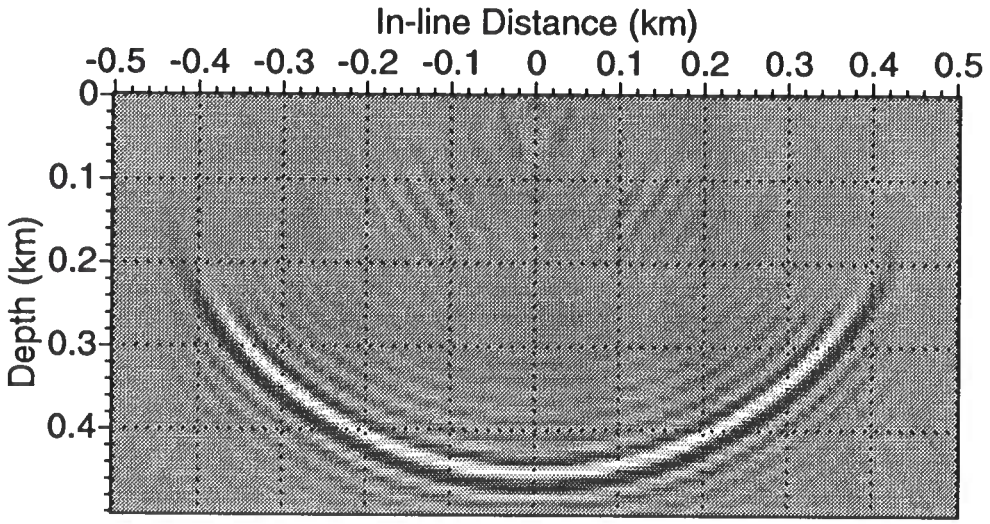

FIG. 24. In-line slice at $y = 0$ from an explicit depth migration of an impulse with a frequency range from 0 to 45 Hz, via Hale's improved McClellan transformation.

- The original hexagonal McClellan transformation is almost as accurate as Hale's improved McClellan transformation, yet it costs less than the original McClellan transformation.
- The improved hexagonal McClellan transformation is more accurate than Hale's improved McClellan transformation, yet it costs about the same.
- Resampling seismic data the hexagonal grid reduces the number of samples that must be repeatedly processed during recursive depth extrapolation.

The one-time costs of resampling data between rectangular and hexagonal grids and creating a new table of 1-D extrapolation filters are insignificant compared to benefits obtained by applying McClellan transformations on hexagonal grids.

ACKNOWLEDGEMENTS

Thanks to my advisor, Dr. Dave Hale, for suggesting this thesis topic and for providing me invaluable guidance and assistance. I would also like to thank the other members of my committee, Dr. Ken Larner and Dr. Ron Knoshaug, for critiquing this thesis and the members of the Center for Wave Phenomena for their input. Financial support for this thesis was given through a fellowship granted by Chevron.

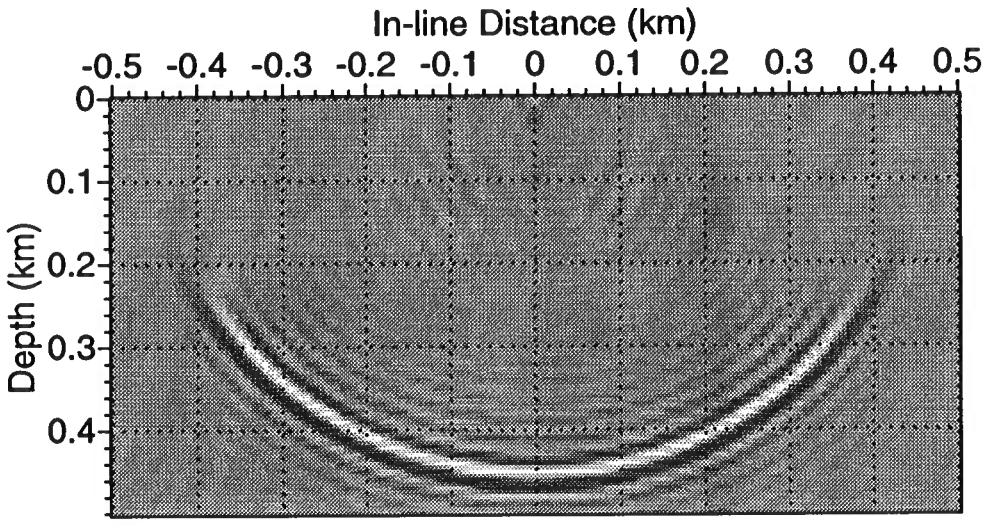

FIG. 25. In-line slice at $y = 0$ from an explicit depth migration of an impulse with a frequency range from 0 to 45 Hz, via the improved hexagonal McClellan transformation.

REFERENCES

Abramowitz, M., and Stegun, I. A., 1965, Handbook of mathematical functions: Dover Publications, Inc.

Blacquière, G., Debeye, H. W. J., Wapenaar, C. P. A., and Berkhout, A. J., 1989, 3D table-driven migration: Geophys. Prosp., **37**, 925–958.

Bracewell, R. N., 1986, The Fourier transform and its applications: McGraw-Hill Book Company.

Brown, D. L., 1983, Applications of operator separation in reflection seismology: Geophysics, **48**, 288–294.

Claerbout, J. F., 1985, Imaging the earth's interior: Blackwell Scientific Publications.

Gazdag, J., 1978, Wave equation migration with the phase-shift method: Geophysics, **43**, 1342–1351.

Hale, D., 1990a, Stable explicit depth extrapolation of seismic wavefields: **CWP-095**, Colorado School of Mines.

Hale, D., 1990b, 3-D depth migration via McClellan transformations: **CWP-096**, Colorado School of Mines.

Holberg, O., 1988, Towards optimum one-way wave propagation: Geophys. Prosp., **36**, 99–114.

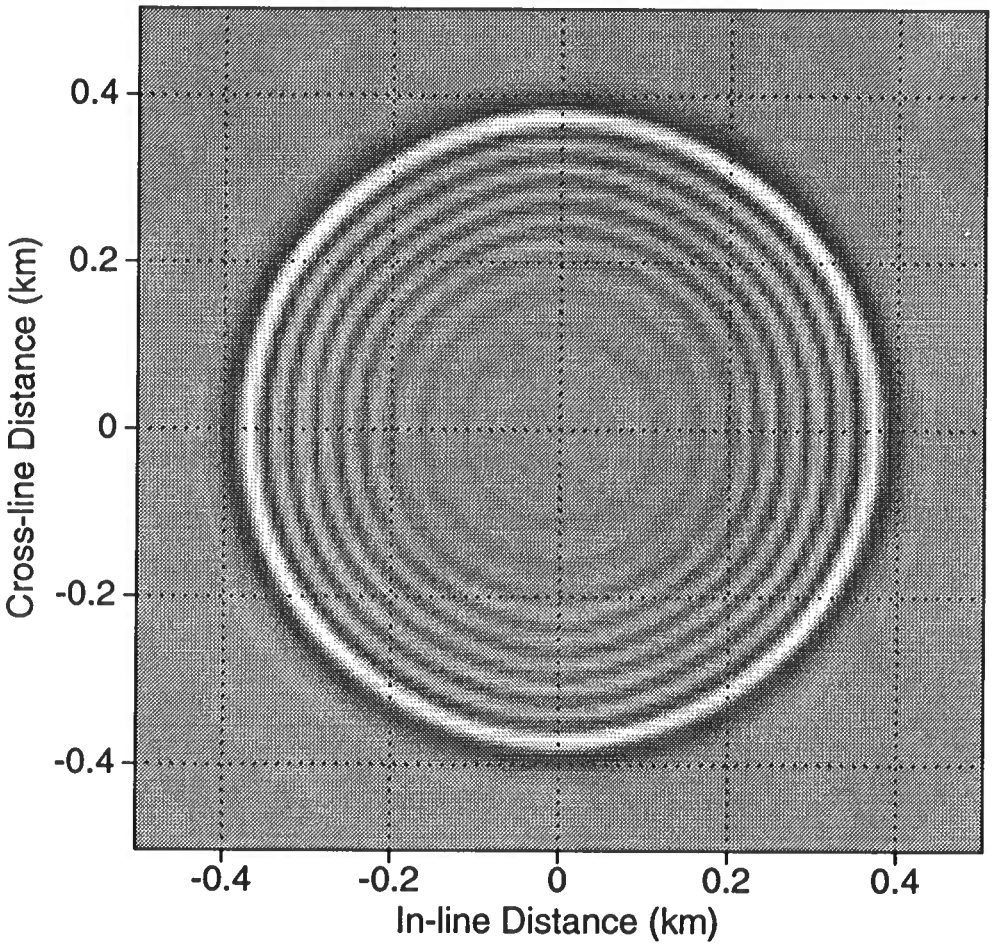

FIG. 26. Depth slice at $z = 250$ m from an explicit depth migration of an impulse with a frequency range from 0 to 45 Hz, via the original hexagonal McClellan transformation.

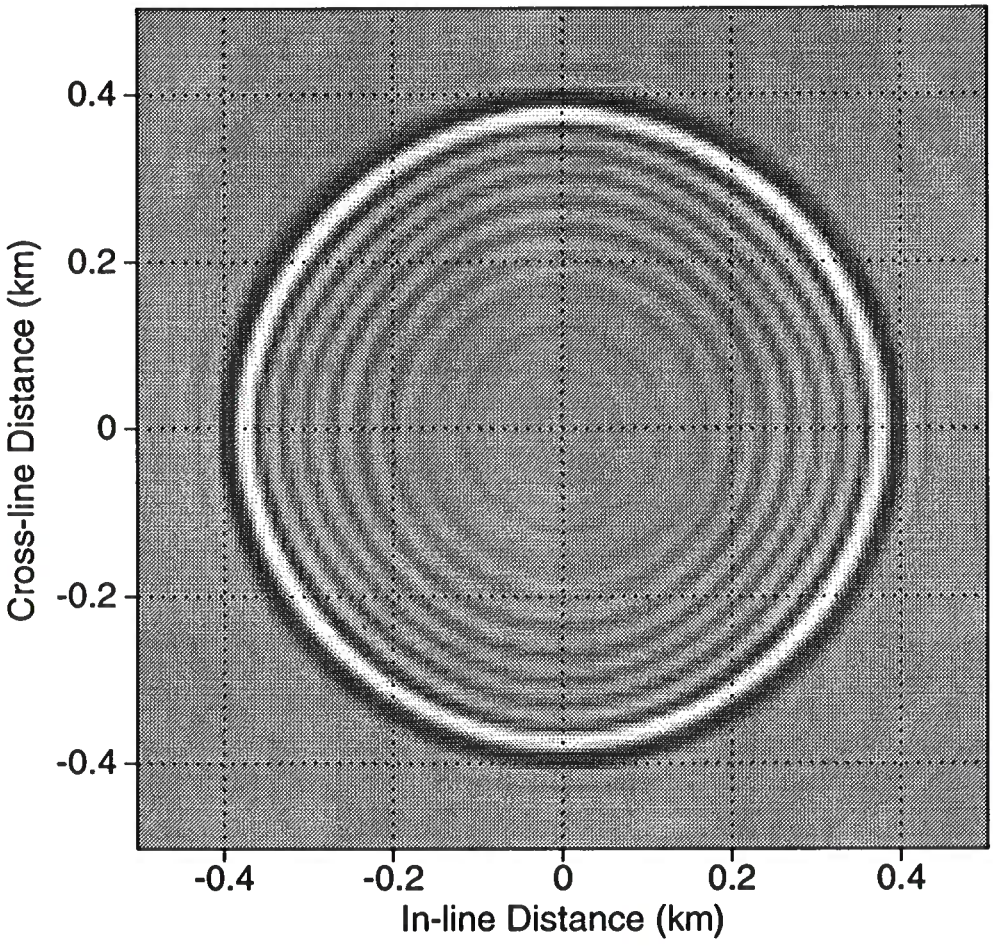

FIG. 27. Depth slice at $z = 250$ m from an explicit depth migration of an impulse with a frequency range from 0 to 45 Hz, via Hale's improved McClellan transformation.

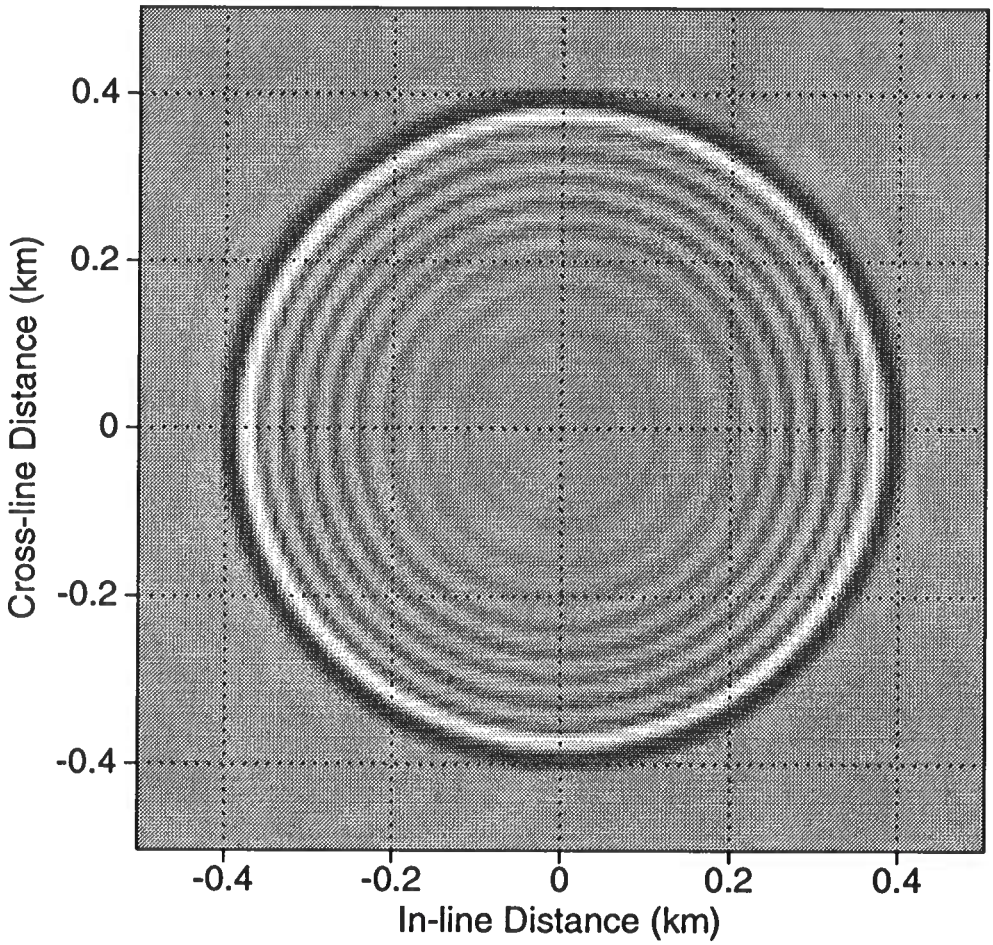

FIG. 28. Depth slice at $z = 250$ m from an explicit depth migration of an impulse with a frequency range from 0 to 45 Hz, via the improved hexagonal McClellan transformation.

Li, Z ., 1991, Compensating finite-difference errors in 3-D migration and modeling: **CWP-099**, Colorado School of Mines.

McClellan, J. H., 1973, The design of two-dimensional digital filters by transformations: Proc. 7th Annual Princeton Conf. on Inform. Sci. and Syst., 247-251.

McClellan, J. H., and Chan, D. S., 1977, A 2-D FIR filter structure derived from the Chebyshev recursion: IEEE Trans. Circuits Syst., **CAS-24**, 372–378.

Mersereau, R. M., Mecklenbräuker, W. G., and Quatieri, T. F., 1976, McClellan transformations for two-dimensional digital filtering: I — design: IEEE Trans. Circuits Syst., **CAS-23**, 405–414.

Mersereau, R. M., 1979, The processing of hexagonally sampled two-dimensional signals: IEEE Proc., **VOL. 67**, 930–949.

Mersereau, R. M., Mecklenbräuker, W. G., and Quatieri, T. F., 1976, McClellan transformations for two-dimensional digital filtering: I — design: IEEE Trans. Circuits Syst. **CAS-23**, 405–414.

Ristow, D., 1980, 3-D downward extrapolation of seismic data, in particular by finite difference methods: PhD thesis, University of Utrecht, The Netherlands.

Yilmaz, O., 1987, Seismic data processing: Soc. of Expl. Geophysics.

APPENDIX A: UNSTABLE 2-D FILTER DESIGNED BY MCCLELLAN TRANSFORMATIONS

Parameter D' in equation (9) was modified to force the outermost contour to match along the diagonal, $k_x = k_y$, at $.9\pi$ which produces the highly circular mapping of Figure 29. However a region exist for which the contours are undefined; that is, the approximation in the region exceeds unity, for which the arcsin is undefined. The modified original McClellan transformation would be ideal since it would significantly increase the accuracy of 2-D extrapolation filters without any increase in computational cost.

Unfortunately, the modified McClellan transformation will produce an unstable depth extrapolation of 3-D wavefields. Equation (9) was used to create the 2-D Fourier transform of a filter designed from the modified McClellan transformation. A simple 19 coefficient 1-D filter for which all coefficients, $h[n] = 1/19$ was used. The maximum magnitude of the 2-D Fourier transform, $H(k_x, k_y)$ should be unity at $k_x = k_y = 0$. However, Figure 30 shows that in the region for which the contours are not defined, the magnitude of the 2-D Fourier transform greatly exceeds unity. Repeated application of these filters will result in the unstable extrapolation of a 3-D wavefield.

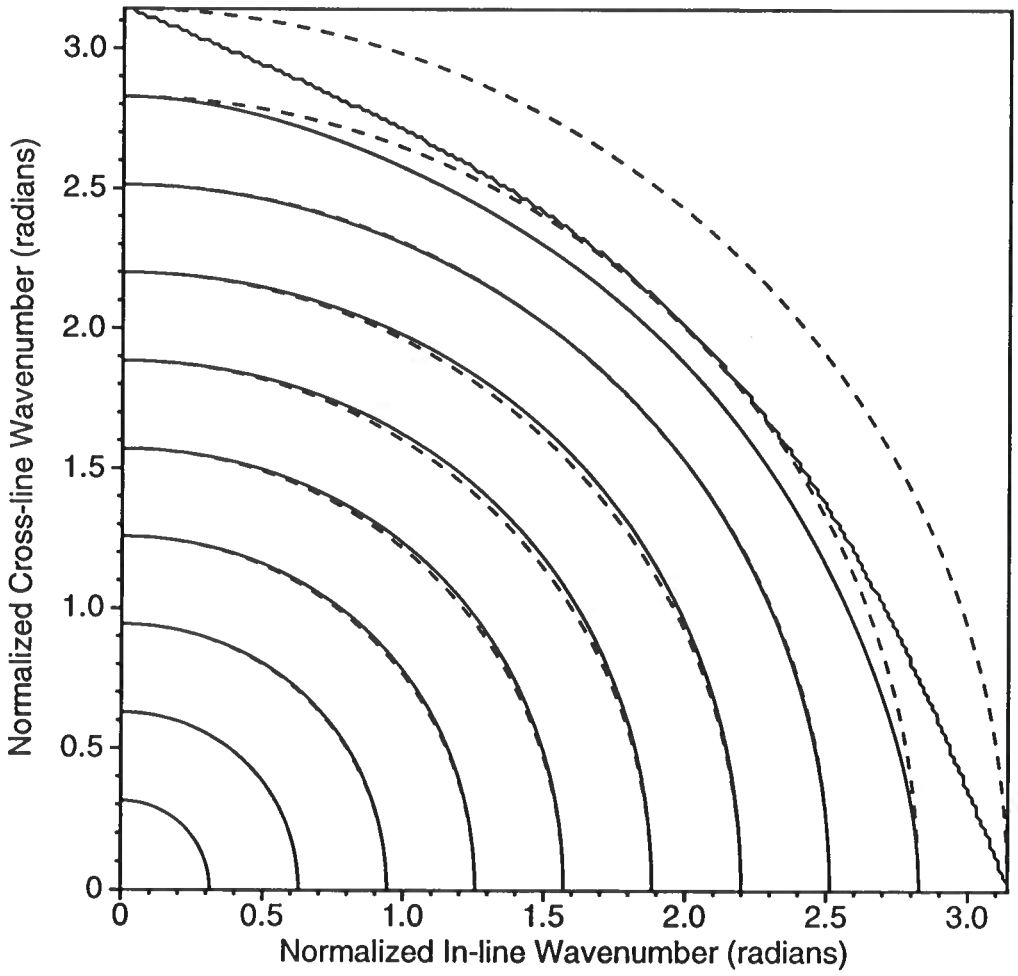

FIG. 29. The modified original McClellan transformation maps the wavenumber response of the 1-D filter to the second dimension along the solid contours. Dashed contours represent an exact circular mapping. Note the region (upper right of wiggly line) for which the contours are undefined.

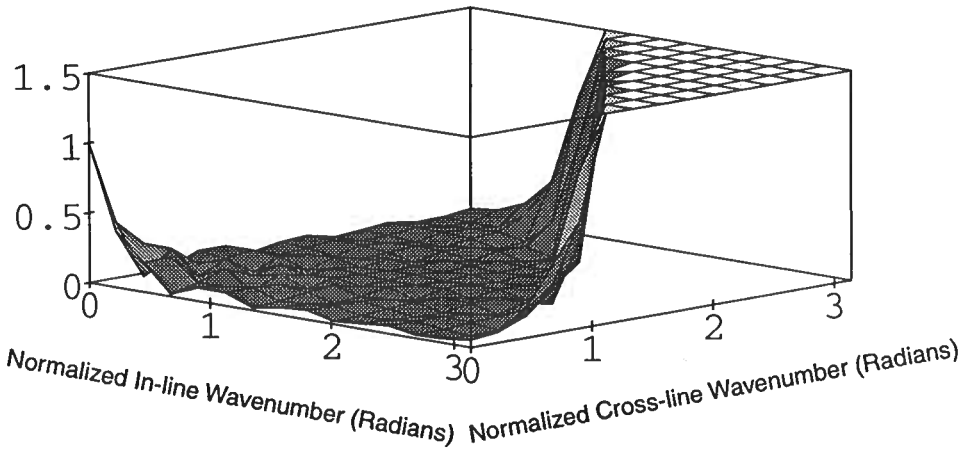

FIG. 30. Fourier transform of a 2-D filter using the McClellan transformation that created Figure 29. Note that the magnitude of the 2-D Fourier transform of the filter undesirably exceeds unity for large k_x and k_y.